Roles of Surface Te, Nb, and Sb Oxides in Propane Oxidation to Acrylic Acid over Bulk Orthorhombic Mo−V−O Phase

Vadim V. Guliants,* Rishabh Bhandari, Balasubramanian Swaminathan, and Vijay K. Vasudevan

Department of Chemical and Material Engineering, University of Cincinnati, Cincinnati, Ohio 45221-0012

Hidde H. Brongersma and Arie Knoester

Calipso B.V. and Department of Applied Physics, Eindhoven University of Technology, P. O. Box 513, 5600 MB Eindhoven, The Netherlands

Anne M. Gaffney† and Scott Han

Rohm and Haas Co., 727 Norristown Road, Spring House, Pennsylvania 19477-0904

Received: August 17, 2005; In Final Form: October 4, 2005

The outermost surfaces and subsurface layers of the orthorhombic (M1) Mo−V−O catalysts promoted with Te, Nb, and Sb oxide species at submonolayer surface coverage were examined by low-energy ion scattering (LEIS). This study indicated that the Nb oxide species was preferentially located at the topmost surface, while the subsurface Te and Sb concentrations declined gradually into the bulk. Although the original Mo−V−O catalyst was essentially unselective in propane oxidation to acrylic acid, significant improvement in the selectivity to acrylic acid was observed when Te, Nb, and Sb oxides were present as the surface species at submonolayer coverage. These findings further suggested that the formation of the surface V−O−M bonds (M = Nb, Te, or Sb) was highly beneficial for both the activity and selectivity of the orthorhombic Mo−V−O catalysts in propane oxidation to acrylic acid. The highest selectivity was observed when both Nb and Te (or Sb) oxide species were present at the surface. The selectivity trends established for the surface-promoted Mo−V−O catalyst parallel those found previously for the corresponding bulk Mo−V−M−O catalysts. These results further indicated that the introduction of surface metal oxide species is a highly promising method to prepare well-defined model catalysts for studies of the structure−activity/selectivity relationships as well as optimize the catalytic performance of the bulk mixed Mo−V−M−O catalysts for selective (amm)oxidation of propane.

Introduction

The current abundance and low environmental impact of propane as a feedstock have generated considerable interest in oxidative catalytic conversion of propane to acrylic acid and acrylonitrile.[1−17] Recently discovered multicomponent Mo−V−Te(Sb)−Nb−O catalysts have shown great promise in propane oxidation to acrylic acid and ammoxidation to acrylonitrile.[4−11,18−24] These mixed-phase catalysts contain so-called "M1" and "M2" phases with orthorhombic and pseudohexagonal structures, respectively, proposed to be active and selective in propane oxidation to acrylic acid and ammoxidation to acrylonitrile.[12−16,20,25−29] In particular, the presence of the M1 phase in these catalysts is associated with their ability to activate propane selectively into acrylic acid and acrylonitrile.[16,18,20,28−31] A recent low-energy ion scattering (LEIS) study of the M1 phases with the bulk Mo−V−Te−O compositions indicated that the surfaces of these catalysts are terminated with a monolayer, which possesses a different elemental composition from that of the bulk.[32] The rates of propane consumption and formation of propylene and acrylic acid depended on the topmost surface V concentration, whereas no dependence of these reaction rates on either the surface Mo or Te concentrations was observed. These findings suggested that the bulk Mo−V−Te−O structure may function as a support for the unique active and selective surface monolayer in propane oxidation to acrylic acid.

In this study we further examined the bulk microstructure, surface chemistry, and catalytic behavior of the M1 phase with a binary metal oxide Mo−V−O composition promoted with Te, Nb, and Sb oxide species at submonolayer surface coverages. The goal of this study was to establish the selectivity trends in propane oxidation over the M1 phase catalysts when the Te, Nb, and Sb oxides were present only as the surface species, because the M1 phase Mo−V−O catalyst used as a support in this study was previously reported to be unselective to acrylic acid.[31,33,34] Therefore, the unique advantage of this catalytic system was that it enabled isolating and studying the effect of one parameter only, namely the nature of the surface metal oxide. While the original Mo−V−O catalyst was essentially unselective in propane oxidation to acrylic acid, significant improvement in the selectivity to acrylic acid was observed when these promoters were present at submonolayer coverage. These findings further suggested that the formation of the surface V−O−M bonds (M = Nb, Te, or Sb) was highly beneficial for

* Corresponding author: Tel +1 513 556 0203; Fax +1 513 556 3473; e-mail vadim.guliants@uc.edu.

† Present address: ABB Lummus Global Inc., Technology Development Center, 1515 Broad Street, Bloomfield, NJ 07003.

10.1021/jp054641y CCC: $30.25
Published on Web 11/23/2005

TABLE 1: Preparation of Promoted Mo−V−O Catalysts

catalyst	coverage	element(s)	element 1 (wt %)	element 2 (wt %)
Mo−V−O, 1 g	monolayer, single	Te	2.9	
Mo−V−O, 1 g	monolayer, single	Nb	3.4	
Mo−V−O, 1 g	monolayer, single	Sb	2.6	
Mo−V−O, 1 g	monolayer, mixed	Te + Nb	1.4 (Te)	1.7 (Nb)
Mo−V−O, 1 g	monolayer, mixed	Sb + Nb	1.3 (Sb)	1.7 (Nb)

the activity and selectivity of the Mo−V−O catalysts for propane oxidation to acrylic acid.

Experimental Section

The mixed Mo−V−O catalysts were prepared hydrothermally using ammonium paramolybdate (Alfa Aesar, 81−83% as MoO_3) and vanadyl(IV) sulfate (Alfa Aesar, 99.9%) as the metal oxide sources according to a reported procedure.[31,33,34] In a typical synthesis, ammonium paramolybdate (Alfa Aesar), 11.5 g, was dissolved in 35 mL of deionized water while stirring at room temperature. Vanadyl sulfate (Alfa Aesar), 8.7 g in 25 mL of deionized water, was added dropwise to the Mo solution under stirring. The resultant dark brown gel was placed in a Teflon-lined stainless steel autoclave and heated for 20 h at 175 °C. The black solid was filtered and dried at 80 °C for 12 h. The black solid was filtered, washed with deionized water, and dried for 12 h at 80 °C. This mixed metal oxide precursor was calcined at 500 °C for 2 h under flowing N_2 (40−60 cm^3/min) in a tubular furnace. The temperature was ramped to 500 °C at 5 °C/min^{-1}.

The Nb, Te, and Sb oxide promoters were introduced at a theoretical monolayer coverage corresponding to 7.5 MO_x/nm^2 [35] of the original Mo−V−O catalyst by incipient impregnation of metal isopropoxide (Alfa Aesar) solutions in anhydrous 2-propanol (Alfa Aesar) in a low-humidity N_2-purged glovebox (Table 1). The details of insipient impregnation procedure may be found elsewhere.[36] The promoted Mo−V−O catalyst were dried overnight in a glovebox under controlled humidity conditions and calcined in N_2 at 500 °C for 2 h.

Propane oxidation was conducted at 350−450 °C using a 48 mL/min feed of 6.3 vol % propane, 9.4 vol % oxygen, 47.3 vol % water vapor, and balance of He and 1.0 g of catalyst packed in a $^3/_8$ in. quartz tubular microreactor in a programmable oven. An HP 5890II gas chromatograph equipped with a Porapak QS 80/100, 6 ft × $^1/_8$ in. × 0.085 in. AT-steel column (Alltech) was employed for the analysis of propane and partial oxidation products by FID, i.e., acrylic acid, propylene, and acetic acid, and a Carbosphere 80/100, 10 ft × $^1/_8$ in. × 0.085 in. SS column (Alltech) for the CO, CO_2, and O_2 analysis by TCD. The lines running from the reactor to the HP 5890II gas chromatograph were kept at 170 °C to prevent condensation of partial oxidation products. The carbon balances agreed within 5 mol %.

The original and promoted Mo−V−O catalysts were characterized by powder X-ray diffraction (XRD) employing Siemens D500 diffractometer (Cu Kα radiation). The SEM images were collected using Hitachi S-900 scanning electron microscope. Transmission electron microscopy (TEM) was performed at the Argonne National Laboratory using a Philips CM30 transmission electron microscope operated at 200 kV with a useful limit of information of 0.14 nm. For TEM, the Mo−V−O catalyst was embedded in epoxy resin, cut to 50−70 nm thick sections, and deposited from dimethyl sulfoxide onto a holey carbon film. The ICP elemental composition was determined using a Leeman Labs ICP/Echelle spectrometer, model PS1000 ICP, equipped with a Hildebrand Grid nebulizer and Mo, V, Te, Nb, and Sb elemental standards (Alfa Aesar). The BET surface areas were determined from the N_2 adsorption isotherms ($0.05 < P/P_0 < 0.3$) at −196 °C employing a Micromeritics TriStar 3000 porosimeter.

The LEIS analysis of model catalysts after kinetic studies was performed employing a Calipso LEIS system equipped with a highly sensitive double-toroidal analyzer (3000× that of other LEIS analyzers). The unique feature of this LEIS system is that the damage inflicted upon the surface is negligible due to the low ion doses.[37] The analysis was performed with both $^4He^+$ and $^{20}Ne^+$ ions at 3 and 5 keV, respectively, as described previously[32] in order to quantify the contributions of the surface O, Mo, V, Te, Nb, and Sb ions. The following surfaces were analyzed: (1) the original surfaces after kinetic studies, (2) the surfaces after treatment with atomic oxygen for 10 min to remove carbonaceous deposits and environmental contaminants, and (3) the surfaces after sputtering of ca. 1 and 3 atomic layers (ML) with 5 keV Ne^+ ions.

The MoO_3, V_3O_5, TeO_2, Nb_2O_5, and Sb_2O_5 standards were also analyzed by LEIS in order to determine the surface metal oxide concentrations in the promoted Mo−V−O catalysts. These metal oxides were treated with atomic oxygen for 10 min and analyzed with 3 keV $^4He^+$ and/or Ne^+ ions. The thus-obtained surfaces were used as "visibility" standards for the metal cations in the outermost surface of the catalysts. These standard surfaces were then sputtered with 5 keV Ne^+ ions to remove ∼1 and 3ML and again measured with 3 keV $^4He^+$ and/or Ne^+ ions. These surfaces were used as indicators of the "visibility" of the metal cations in the subsurface layers of the catalysts at depths of 1 and 3 ML.

Results and Discussion

Synthesis, Phase Composition, and Microstructure of Mo−V−O Catalysts. The formation of the orthorhombic (M1) Mo−V−O phase was investigated over a range of synthesis Mo/V ratios from 1 to 4. The mixed metal oxide precursor phases isolated after 20 h of hydrothermal synthesis were calcined at 500 °C in N_2 to obtain the final Mo−V−O catalysts. The catalysts prepared at the synthesis Mo/V ratios of 1 and 4 showed the presence of impurity phases, mainly MoO_3 (JCPDS 76-1003) and other mixed Mo−V−O phases,[33] together with the orthorhombic M1 phase. The synthesis molar Mo/V ratio ∼ 2 was found to be optimal for the formation of the orthorhombic phase (Figure 1). The major XRD reflections of the M1 and M2 phases can be indexed on the basis of the crystal structures reported recently[29] in the following fashion (2Θ (*hkl*)):

M1: 6.6° (020), 7.8° (120), 9.0° (210), 10.8° (130), 13.0° (310), 22.1° (001), 26.6° (370), 26.9° (550), 27.2° (630), 28.0° (280), 29.1° (560), 31.3° (730), 34.9° (371), 36.0° (281), and 45.2° (002).

M2: 14.0° (200), 22.1° (001), 23.2° (101), 25.3° (120), 26.3° (201), 28.2° (400), 33.1° (311), 36.1° (401), and 45.3° (002).

The pure orthorhombic (M1) phase Mo−V−O catalyst calcined at 500 °C in N_2, possessing the synthesis Mo/V = 2 (i.e., $Mo_6V_3O_x$) and the BET surface area of 6.6 m^2/g, was selected for the study of the Nb, Te, and Sb promoter effects. The XRD pattern of the Mo/V = 2 catalyst treated in N_2 at 500

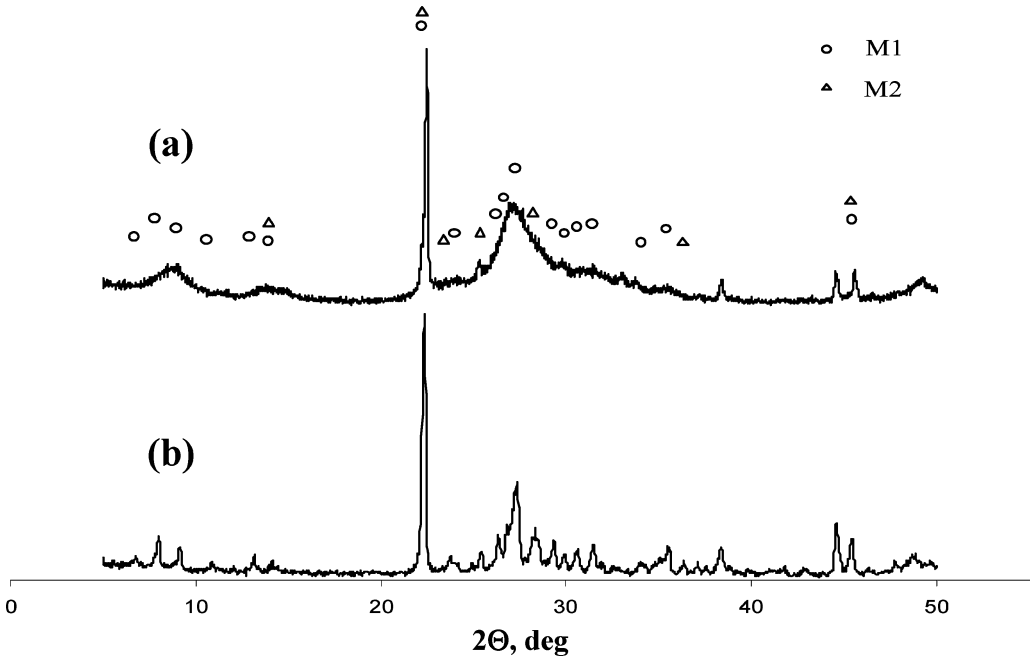

Figure 1. XRD patterns of the (a) Mo−V−O (a) and (b) Mo−V−Te−Nb−O catalysts. The peaks at ∼38.5° and 44.5° 2Θ are those of the Al sample holder.

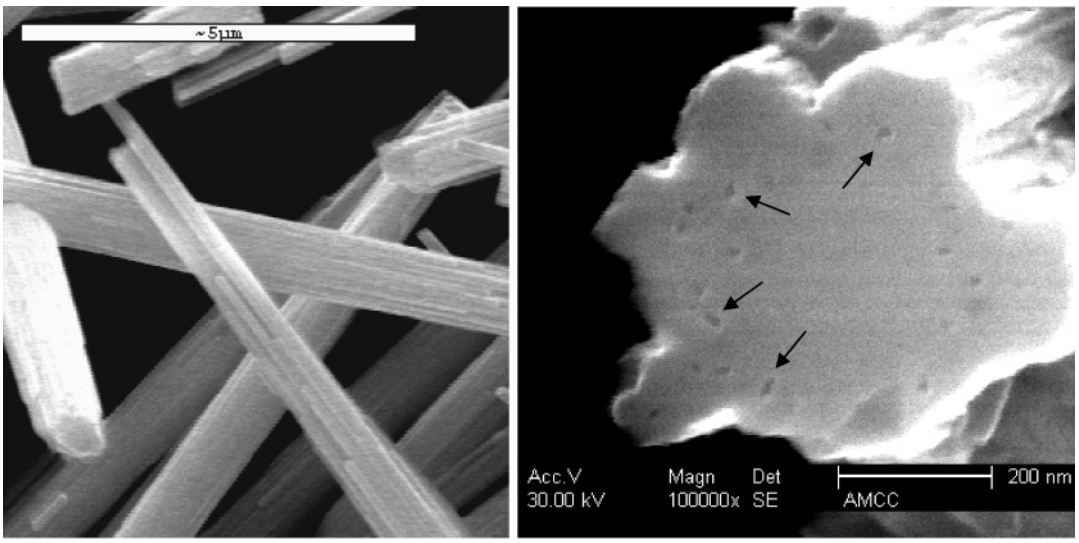

Figure 2. Morphology of the Mo−V−O catalyst after calcination at 500 °C in N_2: (a) rodlike crystals of the M1 phase (scale bar = 5 μm) and (b) high magnification image of the rod end showing numerous nanoscale pits indicated by arrows (scale bar = 200 nm).

°C is shown in Figure 1 together with that of well-crystallized M1 phase containing only traces of the M2 phase (Figure 1b). The XRD pattern of the Mo/V = 2 catalyst (Figure 1a) corresponded to that of less ordered M1 phase due to preferential crystallization of the M1 phase along the *c*-direction which coincided with the long axis of the rodlike crystals of this Mo−V−O catalyst (Figure 2). The SEM analysis showed that these rodlike crystals were 10−20 μm long and 0.3−1 μm thick (Figure 2a). The SEM image of this catalyst collected at a higher magnification (Figure 2b) further revealed the presence of small pits on the top surface of the rodlike crystal. The origin of these pits became apparent after we conducted a high-resolution TEM study of thin sections of this catalyst embedded into epoxy glue. The bright field (BF) TEM image and corresponding selected area electron diffraction (SAED) pattern are shown in Figure 3a,b. The d_{hkl} values calculated from the SAED pattern shown in Figure 3b matched those of the M1 phase.[29] These images demonstrated that the *ab* planes in the M1 phase are oriented perpendicular to the long axis of the rodlike crystal which is coincident with the *c*-direction in the M1 crystal. Moreover, these rodlike crystals are polycrystalline and possess a complex architecture built from nanosized M1 crystallites. The observation of regular areas of low and high contrast visible in Figure 3a suggested that many M1 crystallites are missing, which is probably related to particular conditions during the synthesis of these mixed metal oxides. This conclusion is confirmed by the TEM image of the rodlike crystal collected for the *ab* cross-sectional view shown in Figure 3c. This cross-sectional image shows two types of bright areas: large gaps corresponding to missing crystallites and much smaller gaps which probably correspond to grain boundaries.

The elemental composition of the original Mo−V−O catalyst was determined by ICP to be $Mo_{0.69}V_{0.31}O_x$, which is close to its synthesis composition with a slightly lower V content. The

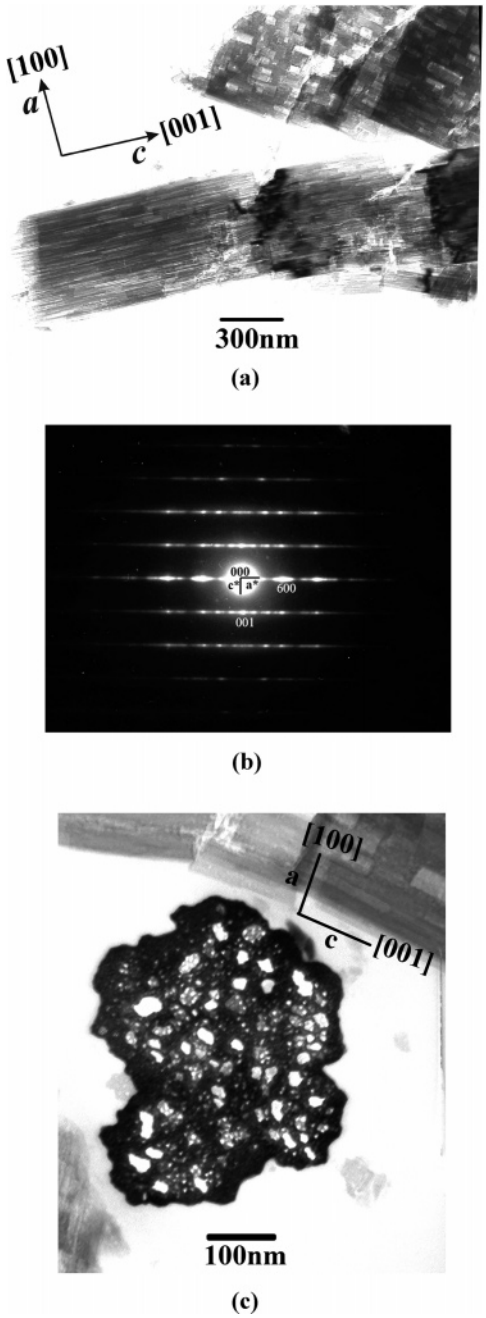

Figure 3. (a) BF micrograph showing rodlike crystals of the M1 phase, (b) corresponding 010 SAED recorded from these particles and (c) BF micrograph showing cross-sectional view of the rodlike M1 crystal.

TABLE 2: ICP Analysis of Promoted Mo−V−O Catalysts[a]

	loadings, wt %		
promoter(s)	Te	Nb	Sb
Te	1.74 (0.60)		
Nb		1.51 (0.44)	
Sb			1.89 (0.73)
Te + Nb	0.63 (0.45)	0.53 (0.31)	
Sb + Nb		0.78 (0.46)	1.18 (0.91)

[a] Fractional monolayer coverages are shown in parentheses.

total content of Nb, Te, and Sb in the promoted Mo−V−O catalysts by ICP was lower than the amounts used in incipient impregnation (Tables 1 and 2) because some of the promoter solution apparently remained on the walls of the container during impregnation. The promoted Mo−V−O catalysts after thermal treatment in N_2 did not show any new crystalline phases besides the M1 phase.

Catalytic Behavior of Mo−V−O Catalysts in Propane Oxidation. The original Mo−V−O catalyst showed low selectivity to acrylic acid (∼4 mol %) and moderate selectivity to propylene (up to 25 mol % at 380 °C) at low propane conversion (Table 3 and Figure 4), in agreement with previous observations.[31,33,34] This catalyst after impregnation with neat 2-propanol showed similarly low selectivity to acrylic acid and slightly increased selectivity to acetic acid. After impregnation with TeO_x at a submonolayer coverage, the selectivity to acrylic acid increased to ∼10 mol % while the selectivity to propylene decreased to ∼10 mol %. The addition of NbO_x and SbO_x to the original Mo−V−O catalyst was more beneficial than that of TeO_x. The NbO_x and SbO_x species had a very similar effect on propane oxidation. The presence of these metal oxides resulted in increased selectivity to acrylic acid (∼15−20 mol %) and propylene (20−30 mol %) and much lower selectivity to complete oxidation products (Table 3). However, when these elements were introduced as pairs, i.e., (Te + Nb) and (Sb + Nb), the improvement in the catalytic behavior was even more significant. The selectivities to acrylic acid and propylene were each ∼30 mol % for the (Te + Nb)-promoted catalyst and ∼20 and 30 mol %, respectively, for the (Sb + Nb)-promoted catalyst. The (Te + Nb)-promoted catalyst showed higher selectivity to acrylic acid than acetic acid, while other model Mo−V−O catalysts of this study were comparably selective to both acids. The effect of the surface TeO_x was manifested in the decrease of the selectivity toward propylene and increase in the selectivity to acrylic acid. Therefore, the best promoted Mo−V−O catalyst of this study contained both Nb and Te (or Sb) similar to the best bulk Mo−V−Te(Sb)−Nb−O catalysts reported for the propane oxidation and ammoxidation.[12−16,25−29,31,33]

The reaction rate analysis further suggested that all metal oxide species investigated promoted propane consumption (Figure 5). The Sb-promoted catalyst displayed the highest rates of propane consumption and formation of propylene, acrylic, and acetic acids. Only for two catalysts, namely the Te- and (Te + Nb)-promoted systems, was the rate of acrylic acid formation equal to or slightly higher than the propylene formation rate, indicating that these promoters were highly beneficial in converting propylene to acrylic acid. All surface metal oxides investigated in this study also promoted the formation of acetic acid, although the rate of acetic acid formation in most cases was lower than that of acrylic acid. This suggests that acetic acid may be formed due to the overoxidation of acrylic acid and to some degree by direct oxidation of propane via the C−C or possibly C═C scission in the surface propylene intermediate. Furthermore, the activation energy for the propane consumption over these model Mo−V−O catalysts (Table 4) was found to be in the range of ∼60−125 kJ/mol based on the first-order reaction rates.[38] This range of activation energies is similar to that found earlier for propane oxidation over slurry Mo−V−Te−Nb−O catalyst (60 kJ/mol[39]), hydrothermal Mo−V−Te−Nb−O (65.4 kJ/mol[33]) and Mo−V−Te−O (65.9 kJ/mol[33]) catalysts, and propane oxidation over supported VO_x and MO_x catalysts (99−120 kJ/mol).[40,41] The activation energy for propane oxidation over the original Mo−V−O catalyst (72 ± 5 kJ/mol) agreed well with the value reported in a previous study (68.8 kJ/mol).[33] The activation energy for propane consumption decreased upon promotion with Sb, remained relatively unchanged upon promotion with Nb and (Sb + Nb), and increased appreciably for the Te- and (Te + Nb)-promoted catalysts.

TABLE 3: Selective Oxidation of Propane over Model Mo−V−O Catalysts

T, °C	flow rate, mL/min	C(C_3H_8), mol %	S(C_3H_6), mol %	S(AA), mol %	S(AceA), mol %	S(CO_x), mol %
			a. Original Mo−V−O Catalyst			
360	49.3	3.1	8	4	3	85
380	59.2	1.6	25	4	2	69
400	59.2	4.7	18	4	2	76
420	59.2	9.4	12	3	2	84
			b. Mo−V−O Catalyst Treated with Anhydrous 2-Propanol			
340	49.3	3.4	3	7	9	79
360	49.3	4.8	2	7	8	83
380	49.3	6.8	3	6	7	84
400	49.3	11.4	1	4	5	89
			c. Te-Promoted Mo−V−O Catalyst			
340	49.3	2.6	14	6	6	73
360	49.3	3.5	9	8	6	77
380	64.1	11.3	7	9	6	77
400	74	11.1	5	8	5	82
			d. Nb-Promoted Mo−V−O Catalyst			
340	49.3	3.8	32	11	23	30
360	49.3	7.8	29	15	22	34
380	49.3	10.8	28	15	20	36
400	49.3	13.6	31	20	19	29
			e. (Nb + Te)-Promoted Mo−V−O Catalyst			
360	49.3	2.8	33	28	19	18
380	49.3	4.2	30	29	18	21
400	49.3	10.2	29	29	18	24
420	49.3	15	19	30	20	29
			f. Sb-Promoted Mo−V−O Catalyst			
360	49.3	10	32	10	30	25
380	49.3	8.5	20	14	16	48
400	49.3	18.1	24	19	18	37
420	49.3	15.9	25	15	21	38
			g. (Nb + Sb)-Promoted Mo−V−O Catalyst			
340	49.3	5.3	29	8	15	46
360	49.3	6.1	33	19	21	29
380	49.3	9.9	26	21	21	31
400	49.3	21.4	29	26	23	18

[a] Feed: 6.3 vol % propane, 9.4 vol % oxygen, 47.3 vol % H_2O, and the balance He. AA = acrylic acid, AceA = acetic acid, and CO_x = carbon oxides.

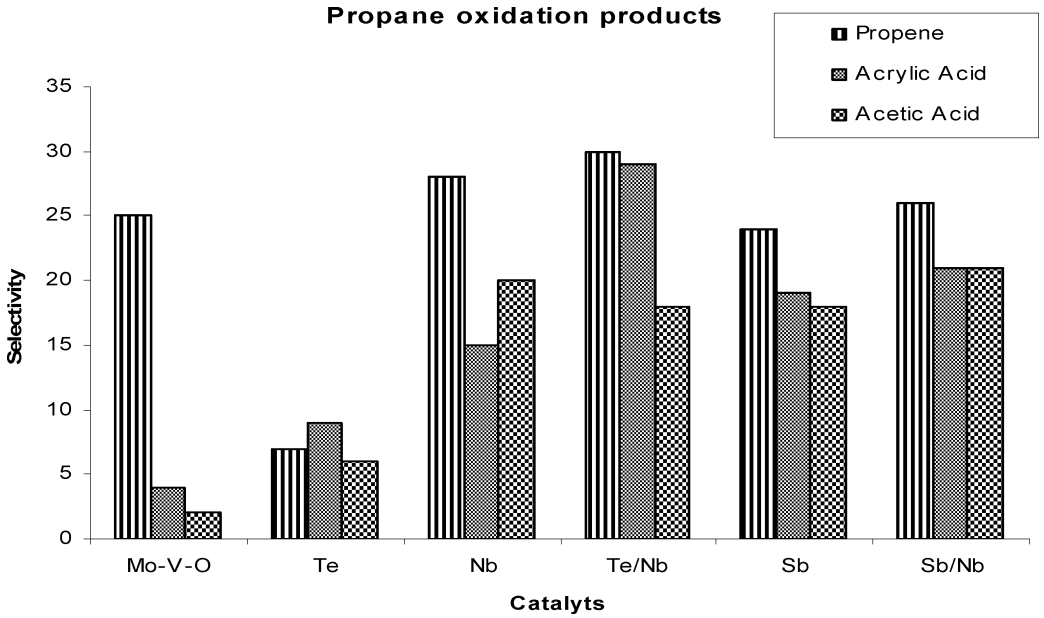

Figure 4. Propane oxidation over model Mo−V−O catalysts at 380°C (from Table 3). Feed: 6.3 vol % propane, 9.4 vol % oxygen, 47.3 vol % H_2O, and the balance He.

Surface Region of Mo−V−O Catalysts. The critical insights into the location and depth profile of the Te, Nb, and Sb oxides came from the LEIS studies. The representative LEIS spectra of the Te-promoted Mo−V−O catalyst are shown in Figure 6, and the (sub)surface atomic fractions of the model Mo−V−O catalysts after kinetic studies are summarized in Table 5. The LEIS spectra of the promoted Mo−V−O catalysts showed the signals originating from O, V, Mo, and the promoter elements

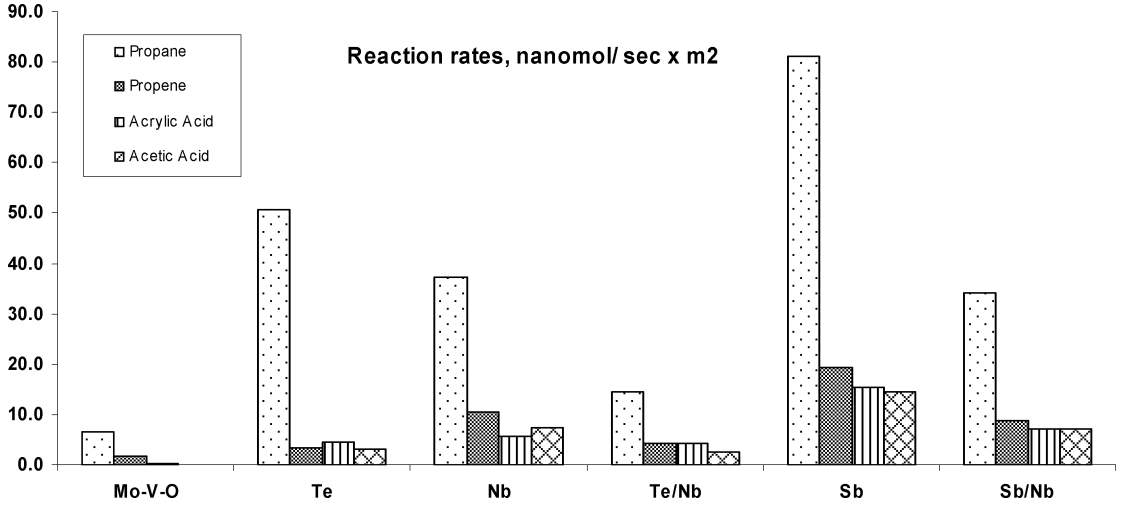

Figure 5. Reaction rates of propane consumption and product formation over model Mo−V−O catalysts at 380 °C. Feed: 6.3 vol % propane, 9.4 vol % oxygen, 47.3 vol % H_2O, and the balance He.

TABLE 4: Activation Energies of Propane Consumption over Mo−V−O Catalysts

promoter	E_a, ±5 kJ/mol	promoter	E_a, ±5 kJ/mol
none	74	Nb	72
Te	125	Nb + Te	108
Sb	62	Nb + Sb	79

as well as environmental contamination in the form of carbonaceous species and surface SiO_x in every promoted catalyst. The SiO_x impurity was apparently present in anhydrous 2-propanol used as-received in the incipient impregnation. This was confirmed by comparing the LEIS spectra of the original Mo−V−O and 2-propanol-treated Mo−V−O catalysts. After the treatment with atomic oxygen, all elemental signals increased due to the removal of environmental contamination and/or product species. The surface SiO_x species was eliminated almost entirely after the removal of one (1 ML) and three (3ML) surface monolayers by Ne^+ sputtering. The LEIS peak areas were calculated using a linear background subtraction procedure for all catalysts and converted to molar elemental compositions corrected for the SiO_x contamination (Table 5).

When compared with its bulk composition, the surface and subsurface layers of the original Mo−V−O catalyst were Mo-enriched (by ∼25%) and V-depleted (by ∼50%). This situation is different from that observed previously in the case of the orthorhombic Mo−V−Te−O catalysts, where Mo depletion and V enrichment were observed in the topmost surface layer.[32] The Mo/V molar ratios determined for the original Mo−V−O catalyst were 5.2 (outermost surface), 7.8 (1 ML), 7.1 (3 ML) and 2.2 (bulk).

The Mo/V molar ratios of the promoted Mo−V−O catalysts followed a similar trend. The Mo/V ratios of the subsurface layers (1 and 3 ML) were always higher than the bulk ratio of 2.2. The Mo/V ratios of the outermost surfaces were always lower than the subsurface ratios. Furthermore, we found clear evidence of (sub)surface enrichment for all promoters investigated. However, these promoters did not form a complete monolayer in the topmost surface. After averaging the promoter concentrations in the surface and subsurface layers, we found the following surface vs bulk enrichment factors: 2.2 (Te), 4.9 (Nb), 2.8 (Sb), 15.2 (Nb), and 2.8 (Te) for the (Nb + Te)-promoted catalyst and 11.2 (Nb) and 1.5 (Sb) for the (Nb + Sb)-promoted catalyst. It is striking that the Nb enrichment factors in these double-promoter catalysts were significantly higher than in the single-promoter systems. Despite their lower

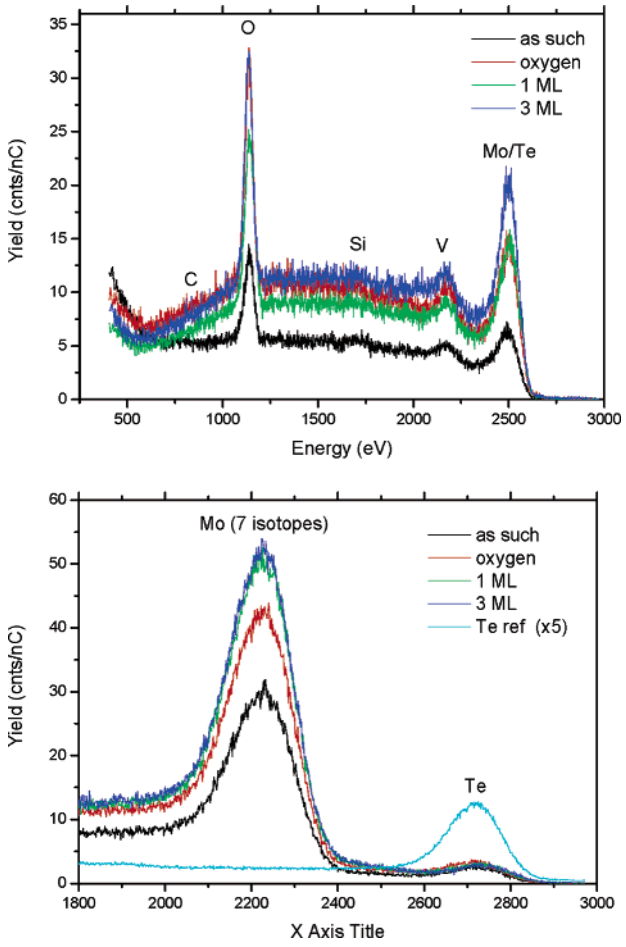

Figure 6. Representative 3 keV $^4He^+$ (top) and 5 keV $^{20}Ne^+$ (bottom) LEIS spectra of the Te-promoted Mo−V−O catalyst. Labels: as such = prior to atomic oxygen treatment; oxygen = atomic oxygen treated; 1 and 3 ML = after sputtering off 1 and 3 ML; Te ref = TeO_2.

bulk Nb concentrations (when compared with the single Nb-promoted catalyst), the (Nb + Te)- and (Nb + Sb)-promoted catalysts showed (sub)surface Nb concentrations that were similar to or slightly higher than that of the Nb-promoted catalyst. The high selectivity of the (Nb + Te)- and (Nb + Sb)-promoted catalysts to acrylic acid (Table 3) may be linked to the high surface enrichment factors found for the Nb promoter.

TABLE 5: LEIS Surface Composition of the Bulk Mo−V−O Catalysts

sample	depth	VO_x (He), mol %	MoO_x (Ne), mol %	NbO_x (Ne), mol %	SbO_x (Ne), mol %	TeO_x (Ne), mol %
Mo−V−O	surface	16.2	83.8			
	1 ML	11.4	88.6			
	3 ML	12.4	87.6			
	bulk(ICP)	31	69			
Mo−V−O	surface	40.8	59.2			
2-propanol	1 ML	22.6	77.4			
	bulk(ICP)	31	69			
Mo−V−O	surface	25.2	70.1			4.6
Te-promoter	1 ML	13.7	82.8			3.5
	3 ML	16.6	80.3			3.1
	bulk(ICP)	30.5	67.8			1.7
Mo−V−O	surface	20.7	70	9.4		
Nb-promoter	1 ML	11.2	79.8	8.9		
	3 ML	12.7	76.3	11.1		
	bulk(ICP)	30.4	67.6	2		
Mo−V−O	surface	15.6	78.5		5.9	
Sb-promoter	1 ML	13.3	81.7		5	
	3 ML	14	80.9		5.1	
	bulk(ICP)	30.4	67.7		1.9	
Mo−V−O	surface	37.3	53.9	6.9		1.9
Nb + Te-promoter	1 ML	23	63.6	11.4		2
	3 ML	16.2	68.9	13.6		1.2
	bulk(ICP)	30.6	68.1	0.7		0.6
Mo−V−O	surface	20.9	68	9.6	1.5	
Nb + Sb-promoter	1 ML	12.8	73.4	11.9	1.9	
	3 ML	11.9	73.8	12.1	2.1	
	bulk(ICP)	30.3	67.5	1	1.2	

[a] Relative (sub)surface fractions ($VO_x + MoO_x + NbO_x + SbO_x + TeO_x = 100\%$).

The two Sb-containing catalysts showed the highest catalytic activity in terms of the rates of propane consumption and formation of propylene, acrylic, and acetic acids (Figure 5). The most active Sb-promoted catalyst possessed not only a higher SbO_x bulk concentration when compared with (Nb + Sb)-promoted catalysts (1.9 vs 1.2%), but it also showed a higher surface vs bulk Sb enrichment (2.8 vs 1.5). Furthermore, these systems had the lowest surface concentrations of carbonaceous species, viz. 20 and 44% respectively for the Sb- and (Nb + Sb)-promoted catalysts. Taking into account that fact that Sb was found to be the most effective *activity* promoter (in terms of the rates of propane consumption and formation of propylene, acrylic acid, and acetic acid), these findings correspond well with the observed activity differences.

Roles of Surface Metal Oxides in Propane Oxidation to Acrylic Acid. We further discussed our findings in light of recent hypothetical models for selective propane (amm)oxidation over the bulk Mo−V−Te−Nb−O catalysts based on the crystal structure of the orthorhombic Mo−V−Te−Nb−O phase.[29,30] According to the model proposed by Grasselli et al.,[30] the active and selective surface sites reside on the bulklike *ab* planes of the M1 phase and consist of an assembly of five metal oxide octahedra, $2V^{5+}/Mo^{6+}$, $1V^{4+}/Mo^{5+}$, $2Mo^{6+}/Mo^{5+}$, and two Te^{4+}−O sites, which are stabilized and structurally isolated from each other by four Nb^{5+} pentagonal-bipyramidal centers. Te^{4+} cations predominantly occupy the hexagonal channels that run along the *c*-axis in the M1 structure. Nb is thought to play two important roles in the M1 structure: (1) by providing site isolation of the active centers from each other, which results in highly selective propane (amm)oxidation, and (2) by stabilizing the crystal structure under catalytic reaction conditions. The propane-activating function of the M1 phase in this model is assigned to the V^{5+} sites of the catalytic center, while the two Te^{4+}−O sites are responsible for the α-H abstraction from the surface propylene intermediate. The resulting π-allyl intermediate is bonded to a neighboring Mo^{6+} of the active center, which is capable of either the NH or O insertion leading to acrylonitrile or acrylic acid (via acrolein), respectively.

In a model proposed by Ueda et al.,[33] the unique ability of the orthorhombic Mo−V−Te−Nb−O catalysts to activate propane selectively is associated with the presence of characteristic heptagonal channels in the M1 structure. In this model, propane is first activated on a Mo−O−V−O−H^+ site located in the surface of the heptagonal channel, which is followed by the allylic oxidation of propylene at the Mo(V)−O−Te−O site associated with the hexagonal channels and concluded by acrolein oxidation to acrylic acid over the former site, i.e., Mo−O−V−O−H^+. Acrylic acid is adsorbed at the surface TeO_x (and NbO_x) site which retards its decomposition.

The results obtained in this study indicated that the NbO_x species were predominantly located at the surface of the model Mo−V−O catalysts, while Sb and, in particular, Te oxide species were present in the subsurface layers at a relatively high concentration. These observations suggested that both Sb and Te oxide species are able to enter the hexagonal and heptagonal channels of the M1 structure of the Mo−V−O catalyst.[12,33] The presence of the surface TeO_x resulted in a significant drop in the selectivity to propylene, suggesting that the surface Te sites are involved in the subsequent oxidation of the surface propylene intermediate.[30,33] Although the surface TeO_x promoted propylene oxidation, its impact on the selectivity to acrylic and acetic acids was modest. This observation is in agreement with recent findings of Ueda et al.,[33] who investigated the oxidation of propane, propene, acrolein, and acrylic acid over hydrothermal Mo−V−O, Mo−V−Te−O, and Mo−V−Te−Nb−O (M1) catalysts. They observed that the presence of the surface TeO_x species was critical only for the step of propylene oxidation to acrolein, while the Mo−V−O catalyst was highly efficient in acrolein oxidation to acrylic acid. By contrast, the surface SbO_x species (Table 3 and Figure 5) were more efficient in promoting propane oxidation to propylene and its further oxidation into acrylic and acetic acids similar to recent observations of propane

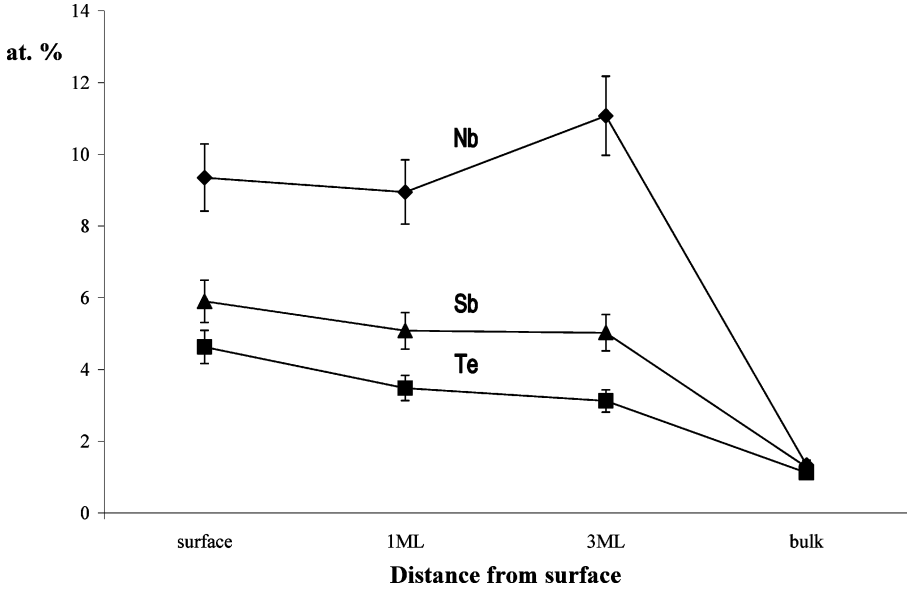

Figure 7. Promoter concentration profiles in the surface region of the model Mo−V−O catalysts promoted with TeO_x, NbO_x, and SbO_x species.

oxidation over the bulk Mo−V−Sb−O catalysts,[42] suggesting that this species plays a role in several reaction steps of propane oxidation.

On the other hand, it appears unlikely that the NbO_x species introduced into the Mo−V−O catalyst by incipient impregnation were able to substitute the Mo and/or V cations occupying the pentagonal-bipyramidal sites in this M1 phase. We further concluded on the basis of the reported M1 crystal structure[29] that both hexagonal and heptagonal channels appear to be too narrow to accommodate the niobium oxide octahedra. Therefore, it is not surprising to observe a much more significant surface Nb enrichment than that observed for the TeO_x and SbO_x species. In this case the surface NbO_x is unlikely to play the site isolation function similar to that proposed for the Nb sites in the orthorhombic Mo−V−Te−Nb−O catalysts.[30] However, it is remarkable that the surface NbO_x species even at a very low concentration had a significant impact on both the activity and selectivity of propane oxidation to acrylic and acetic acids. The observed enhancement of the rate of propane consumption and formation of reaction products in the presence of the surface NbO_x suggested that this metal oxide species plays a role in propane oxidation by forming the surface V−O−Nb (and Mo−O−Nb) bonds in addition to the proposed site isolation and structure stabilization functions.[30] Increased selectivity to propylene, acrylic acid, and acetic acid in the presence of the surface NbO_x suggested that both the Nb and Sb promoters had a similar impact on propane oxidation.

The surface Nb enrichment was much higher when Nb was introduced together with Te or Sb possibly indicating some interaction between these promoter species, which resulted in increased selectivity to acrylic acid. The presence of Te or Sb together with Nb was particularly beneficial for the selectivity to acrylic acid. Ueda et al.[33] observed recently that the hydrothermal orthorhombic Mo−V−Te−Nb−O catalysts displayed much lower rate of acrylic acid decomposition than the orthorhombic Mo−V−O and Mo−V−Te−O catalysts. Furthermore, Wachs et al. recently studied methanol decomposition over hydrothermal Mo−V−O, Mo−V−Te−O, and Mo−V−Te−Nb−O (M1) catalysts and concluded that only the Mo−V−Te−Nb−O catalyst contained the surface acid sites in addition to the redox V^{5+} sites in all three catalysts.[43] Therefore, it appears that another role of surface NbO_x is to provide the surface acid sites which control desorption of acrylic acid and suppress its overoxidation.

Therefore, the present study pointed to the following catalytic functions of the constituent metal oxides in the orthorhombic mixed metal Mo−V−M−O catalysts. The Mo−V−O M1 phase is capable of activating propane; however, it shows low catalytic activity and lacks the surface sites that are able to both bind the propylene intermediate strongly and oxidize it further to acrolein and acrylic acid. The addition of the M = Te, Sb, and Nb oxide species results in the formation of the surface V−O−M (and Mo−O−M) bonds and enhances the rates and selectivity of propane oxidation and formation of partial oxidation products. The surface TeO_x species are important for the allylic oxidation of propylene intermediate, while the surface NbO_x in addition to the site isolation function moderates adsorption of reaction intermediates and products and prevents overoxidation of acrylic acid. Another important conclusion of this study is that the introduction of surface metal oxide species is a highly promising method to prepare well-defined model catalysts for studies of the structure−activity/selectivity relationships as well as optimize the catalytic performance of the bulk mixed Mo−V−M−O catalysts for selective (amm)oxidation of propane.

Conclusions

In this study we investigated the location and roles of the surface Te, Nb, and Sb oxides in selective propane oxidation over the model bulk Mo−V−O catalyst possessing the orthorhombic (M1) structure. These metal oxides are regarded as essential components for selective propane (amm)oxidation over orthorhombic Mo−V−M−O (M = Nb, Te, or Sb) catalysts. We observed a complex nanoscale architecture of the rodlike M1 crystals, in which the *ab* planes proposed to contain the active and selective surface sites[30,33] were aligned normal to the long rod axis. The surface TeO_x, NbO_x, and SbO_x species had a significant impact on the rate and selectivity of propane oxidation over the orthorhombic Mo−V−O catalysts even at low surface coverages. The Te, Nb, and Sb oxide species promoted the rates of propane consumption and formation of propylene, acrylic acid, and acetic acid over the model Mo−V−O catalysts and improved considerably the selectivity to

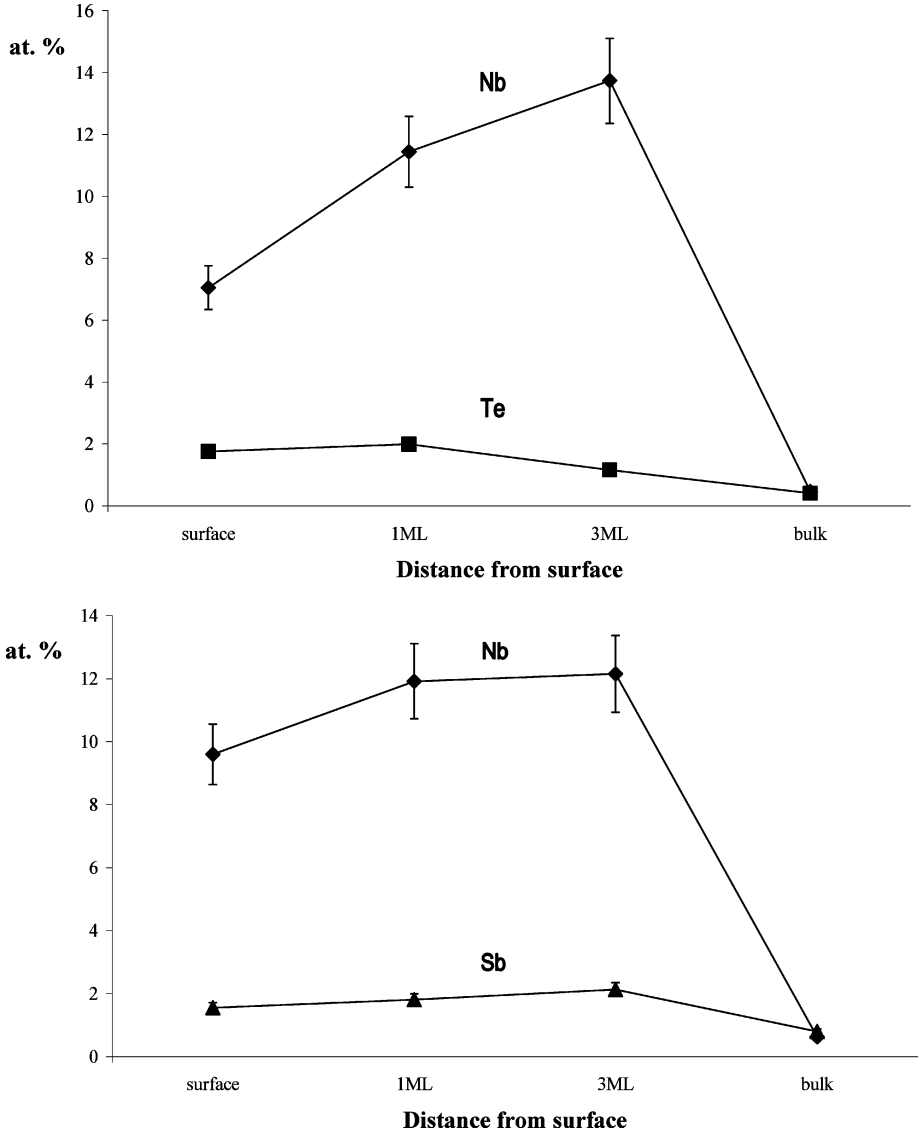

Figure 8. Promoter concentration profiles in the surface region of the model Mo−V−O catalysts containing pairs of promoters: (a) Nb + Te and (b) Nb + Sb.

partial oxidation products. The model Mo−V−O catalyst promoted with pairs of promoters, i.e., Te + Nb and Sb + Nb, displayed the highest selectivities to acrylic acid. These selectivity trends paralleled those observed previously for the bulk mixed Mo−V−M−O catalysts (M = Te, Nb, Sb).

The LEIS study of the model Mo−V−O catalysts revealed that the surface and subsurface layers of the original Mo−V−O catalyst were Mo-enriched and V-depleted, whereas the opposite trend was observed previously in the case of the orthorhombic Mo−V−Te−O catalysts.[32] The NbO_x species were predominantly located at the outermost surface, while Sb and, in particular, Te oxide species penetrated into several subsurface layers of the orthorhombic Mo−V−O phase. These observations suggested that both Sb and Te oxide species are able to enter the hexagonal and heptagonal channels in the orthorhombic Mo−V−O phase.[12,33] The presence of the surface TeO_x resulted in a significant drop in the selectivity to propylene, suggesting that the surface Te sites are involved in the subsequent oxidation of the surface propylene intermediate, in agreement with a recent hypothetical model of propane (amm)oxidation over the bulklike *ab* planes of the M1 phase.[30,33] Although the surface Te did promote propylene oxidation, its impact on the selectivity to acrylic and acetic acids was very modest. By contrast, the surface SbO_x species were more efficient in promoting propane oxidation to propylene and its further oxidation into acrylic and acidic acids, suggesting that this promoter species plays a role in several reaction steps of propane oxidation.

A much more significant surface enrichment was observed for the NbO_x than the TeO_x and SbO_x species probably because the former species was unable to substitute the occupied pentagonal-bipyramidal sites or enter the open channels in the M1 structure. The observed enhancement of the rate of propane consumption and formation of reaction products in the presence of the surface NbO_x suggested that this metal oxide species plays a role in propane oxidation by forming the surface V−O−Nb (and Mo−O−Nb) bonds in addition to the proposed site isolation and structure stabilization functions.[30] The surface Nb enrichment was much higher when Nb was introduced together with Te or Sb, possibly indicating some interaction between these promoter species, which resulted in increased selectivity to acrylic acid. The presence of Te or Sb together with Nb was particularly beneficial for the selectivity to acrylic acid.

Another important conclusion of this study is that the introduction of surface metal oxide species is a highly promising method to prepare well-defined model catalysts for studies of the structure−activity/selectivity relationships as well as opti-

mize the catalytic performance of the bulk mixed Mo−V−M−O catalysts for selective (amm)oxidation of propane.

Acknowledgment. This research was supported by the Chemical Sciences, Geosciences and Biosciences Division, Office of Basic Energy Sciences, Office of Science, U.S. Department of Energy, under Grant DE-FG02-04ER15604. The LEIS study was conducted with financial support of the National Science Foundation (international supplement to NSF CAREER CTS-0238962 to V.V.G.) and Rohm and Haas Co. The authors thank Dr. Rajiv S. Soman (University of Cincinnati) for the ICP elemental analysis of the promoted Mo−V−O catalysts.

References and Notes

(1) Thomas, J. M.; Thomas, W. J. *Principle and Practice of Heterogeneous Catalysis*; VCH Publications: New York, 1987.

(2) Satterfield, C. N. *Heterogeneous Catalysis in Practice*, 2nd ed.; McGraw-Hill: New York, 1991.

(3) Centi, G.; Cavani, F.; Trifirò, F. *Selective Oxidation by Heterogeneous Catalysis*; Kluwer Academic/Plenum Publishers: Norwell, MA, 2001.

(4) Lin, M. *Appl. Catal*. **2001**, *A207*, 1.

(5) Grasselli, R. K. *Catal. Today* **1999**, *49*, 141.

(6) Bettahar, M. M.; Costentin, G.; Savary, L.; Lavalley, J. C. *Appl. Catal*. **1996**, *A145*, 1.

(7) Lin, M. *Appl. Catal.* **2003**, *A250*, 305.

(8) Lin, M. *Appl. Catal.* **2003**, *A250*, 287.

(9) Cavani, F.; Trifirò, F. *Catal. Today* **1999**, *51*, 561.

(10) Cavani, F.; Trifirò, F. *Stud. Surf. Sci. Catal.* **1997**, *110*, 19.

(11) Baerns, M.; Buyevskaya, O. *Catal. Today* **1998**, *45*, 13.

(12) Vitry, D.; Morikawa, Y.; Dubois, J. L.; Ueda, W. *Top. Catal*. **2003**, *23*, 47.

(13) DeSanto, P., Jr.; Buttrey, D. J.; Grasselli, R. K.; Lugmair, C. G.; Volpe, A. F.; Toby, B. H.; Vogt, T. *Top. Catal*. **2003**, *23*, 23.

(14) Grasselli, R. K.; Burrington, J. D.; Buttrey, D. J.; DeSanto, P., Jr.; Lugmair, C. G.; Volpe, A. F., Jr.; Weingand, T. *Top. Catal.* **2003**, *23*, 5.

(15) Holmberg, J.; Grasselli, R. K.; Andersson, A. *Top. Catal.* **2003**, *23*, 55.

(16) Baca, M.; Pigamo, A.; Dubois, J. L.; Millet, J. M. M. *Top. Catal.* **2003**, *23*, 39.

(17) Vitry, D.; Morikawa, Y.; Dubois, J. L.; Ueda, W. *Appl. Catal.* **2003**, *A251*, 411.

(18) Guliants, V. V.; Bhandari, R.; Soman, R. S.; Guerrero-Perez, O.; Banares, M. A. *Appl. Catal.* **2004**, *A274*, 123.

(19) Lin, M.; Linsen, M. W. US Patent 6,180,825, 2001, to Rohm and Haas Co.

(20) Al-Saeedi, J. N.; Vasudevan, V. K.; Guliants, V. V. *Catal. Commun.* **2003**, *4*, 537.

(21) Ushikubo, T.; Koyasu, Y.; Nakamura, H.; Wajiki, S. JP 10045664, 1998, to Mitsubishi Chemical Corp.

(22) Ushikubo, T.; Oshima, K. JP 10036311, 1998, to Mitsubishi Chemical Corp.

(23) Hatano, M.; Kayou, A. European Patent 318,295, 1988, to Mitsubishi Chemical Corp.

(24) Ushikubo, T.; Oshima, K.; Kayo, A.; Umezawa, T.; Kiyona, K.; Sawaki, I. European Patent 529,853, 1992, to Mitsubishi Chemical Corp.

(25) Ushikubo, T.; Oshima, K.; Kayo, A.; Vaarkamp, M.; Hatano, M. *J. Catal.* **1997**, *169*, 394.

(26) Millet, J. M. M.; Roussel, H.; Pigamo, A.; Dubois, J. L.; Dumas, J. C. *Appl. Catal.* **2002**, *A232*, 77.

(27) Aouine, M.; Dubois, J. L.; Millet, J. M. M. *Chem. Commun.* **2001**, *13*, 1180.

(28) Botella, P.; Garcia-Gonzalez, E.; Dejoz, A.; Lopez Nieto, J. M.; Vazquez, M. I.; Gonzalez-Calbet, J. *J. Catal.* **2004**, *225*, 428.

(29) DeSanto, P., Jr.; Buttrey, D. J.; Grasselli, R. K.; Lugmair, C. G.; Volpe, A. F.; Toby, B. H.; Vogt, T. *Z. Kristallogr.* **2004**, *219*, 152.

(30) Grasselli, R. K.; Buttrey, D. J.; DeSanto, P., Jr.; Burrington, J. D.; Lugmair, C. G.; Volpe, A. F., Jr.; Weingand, T. *Catal. Today* **2004**, *91*−*92*, 251.

(31) Katou, T.; Vitry, D.; Ueda, W. *Catal. Today* **2004**, *91*−*92*, 237.

(32) Guliants, V. V.; Bhandari, R.; Brongersma, H. H.; Knoester, A.; Gaffney, A. M.; Han, S. *J. Phys. Chem. B* **2005**, *109*, 10234.

(33) Ueda, W.; Vitry, D.; Katou, T. *Catal. Today* **2005**, *99*, 43.

(34) Ueda, W.; Vitry, D.; Katou, T. *Catal. Today* **2004**, *96*, 235.

(35) Guliants, V. V. *Catal. Today* **1999**, *51*, 255.

(36) Hutchings, G. J.; Vedrine, J. C. *Heterogeneous Catalyst Preparation*; *Springer Ser. Chem. Phys.* **2004**, *75*, 217.

(37) Maas, A. J. H.; Viitanen, M. M.; Brongersma, H. H. *Surf. Interface Anal.* **2000**, *30*, 3.

(38) Balcells, E.; Borgmeier, F.; Grisstede, I.; Lintz, H.-G. *Catal. Lett.* **2003**, *87*, 195.

(39) Balcells, E.; Borgmeier, F.; Grisstede, I.; Lintz, H.-G.; Rosowski, F. *Appl. Catal*. **2004**, *A266*, 211.

(40) Chen, K.; Bell, A. T.; Iglesia, E. *J. Phys. Chem. B* **2000**, *104*, 1292.

(41) Argyle, M. D.; Chen, K.; Bell, A. T.; Iglesia, E. *J. Catal.*. **2002**, *208*, 139.

(42) Concepcion, P.; Botella, P.; Lopez Nieto, J. M. *Appl. Catal., A* **2004**, *278*, 45.

(43) Wachs, I. E.; Jehng, J.-M.; Ueda, W. *J. Phys. Chem. B* **2005**, *109*, 2275.